

Supplementary Information

**An open-cage bis[60]fulleroid as electron transport
material for tin halide perovskite solar cells**

*Wentao Liu,^{‡a} Guanglin Huang,^{‡a} Chien-Yu Chen,^{‡a} Tiancheng Tan,^a Harata Fuyuki^a Shuailfeng Hu,^a
Tomoya Nakumura,^a Minh Anh Truong,^a Richard Murdey,^a Yoshifumi Hashikawa,^a Yasujiro Murata,^{a*}
and Atsushi Wakamiya^{a*}*

*E-mail: yasujiro@scl.kyoto-u.ac.jp, wakamiya@scl.kyoto-u.ac.jp

Author Contributions

W. L., G. H., A.W., and Y.M. conceived the idea; G. H. synthesized and characterized the target compound and carried out UV, MS, HPLC, NMR measurements and DFT calculations; W. L. and C. C. fabricated the solar cell devices and measured the SEM, EQE, ideality factor, and stability; W. L., C. C. and R. M. measured AFM; G. H., T. T., and C. C. conducted CV measurements with the help of M. A. T.; C. C. and G. H. carried out the XPS measurements with the help of T. N. and F. H.; C. C. and G. H. conducted TGA measurements; C. C. and R.M. carried out EIS measurements; C. C. and F. H. conducted PL and TRPL measurements; C. C. carried out SCLC measurements; W. L., G. H., and C. C. prepared the manuscript. A. W., Y. M, R. M., Y. H., T. N., and S. H. edited and reviewed the manuscript; All authors commented on the manuscript; A. W. and Y. M. supervised the project.

Experimental section

Materials

Formamidinium iodide (FAI, 99.99%) and bathocuproine (BCP) were purchased from Tokyo Chemical Industry Co., Ltd. (TCI). Ammonium thiocyanate (NH_4SCN , 99.99% trace metals basis), tin(II) fluoride (SnF_2 , 99%), and tin(II) iodide (SnI_2 , beads, 99.99%, trace metals basis), ethane-1,2-diammonium iodide (ethylenediammonium diiodide, EDAI_2 , $\geq 98\%$), and 1-chloronaphthalene (1-CINp) were purchased from Sigma-Aldrich Co., Ltd. (Sigma-Aldrich). Poly (3,4-ethylenedioxythiophene): poly (styrene sulfonate) (PEDOT:PSS) aqueous solution (Clevious PVP AI 4083) was purchased from Heraeus Co., Ltd. Fullerene C_{60} (sublimed, 99.99%) was purchased from ATR Company and Fullerene C_{60} (95%) for synthesis was purchased from SES Research Co. Phenyl- C_{61} -butyric acid methyl ester (PCBM) and Indene- C_{60} bisadduct (ICBA) was purchased from Ossila. Zinc oxide (ZnO) nanoparticle ink was purchased from Sigma-Aldrich. Dehydrated dimethyl sulfoxide (DMSO, super dehydrated), dehydrated orthodichlorobenzene (ODCB), carbon disulfide (CS_2), dehydrated 1,2,4-trichlorobenzene (TCB), and acetonitrile were purchased from FUJIFILM Wako Pure Chemical Co., Ltd. Dimethylformamide (DMF), toluene, and chlorobenzene were purchased from Kanto Chemical. Co., Inc. Hexane and toluene were purchased from Nacalai Tesque, Inc. All of these solvents that were used for the fabrication of devices were degassed by Ar gas bubbling for 1 h and further dried with molecular sieves (3 Å) in an Ar-filled glove box (H_2O , $\text{O}_2 < 0.1$ ppm) before use. Open-cage bis[60]fulleroid (OC) was synthesized according to the literature.¹ Unless otherwise noted, materials purchased from commercial suppliers were used without further purification. All reactions were carried out under an Ar atmosphere. All the materials were used as received.

Preparation of perovskite films

$\text{PEA}_{0.15}\text{FA}_{0.85}\text{SnI}_3$

0.8 M $\text{PEA}_{0.15}\text{FA}_{0.85}\text{SnI}_3$ perovskite solution was prepared by dissolving PEAI (30.0 mg, 0.12 mmol), FAI (116.9 mg, 0.68 mmol), SnI_2 (298.0 mg, 0.8 mmol) SnF_2 (9.4 mg, 0.06

mmol) and NH_4SCN (3.0 mg, 0.04 mmol) in a mixed solvent of 0.8 mL DMF and 0.2 mL DMSO. The precursor solution was stirred at 70 °C for 1 h and filtered through a 0.20 μm PTFE filter before spin-coating. After the precursor solution was cooled down to room temperature, 100 μL of the precursor solution was spin-coated at 5000 rpm for 50 s with an acceleration of 1000 rpm s^{-1} (total time for spin-coating is 55 s). 500 μL of toluene antisolvent was dripped onto the surface of the spinning substrate at 52 s during the spinning. Then, the substrate was immediately annealed on a 70 °C hot plate for 10 min. All the steps above were conducted in an Ar-filled glove box (H_2O , $\text{O}_2 < 0.1$ ppm).

$\text{FA}_{0.75}\text{MA}_{0.25}\text{SnI}_3$

1.0 M $\text{FA}_{0.75}\text{MA}_{0.25}\text{SnI}_3$ perovskite solution was prepared by dissolving FAI (129.0 mg, 0.75 mmol), MAI (39.8 mg, 0.25 mmol), SnI_2 (372.6 mg, 1.0 mmol) and SnF_2 (15.7 mg, 0.1 mmol) in 1.0 mL DMSO. The precursor solution was stirred at 45 °C for 1.5 h and filtered through a 0.20 μm PTFE filter before spin-coating. After the precursor solution was cooled down to room temperature, 200 μL of the precursor solution was spin-coated at 5000 rpm for 60 s with an acceleration of 1000 rpm s^{-1} . 300 μL chlorobenzene (preheated to 65 °C) was used as antisolvent and dripped slowly onto the surface of spinning substrate at 2 s during the spin-coating step. The substrate was immediately annealed at 65 °C for over 10 min and then 100 °C for 10 min. All the steps above were conducted in an Ar-filled glove box ($\text{H}_2\text{O} < 0.1$ ppm, $\text{O}_2 < 0.1$ ppm).

Device fabrication

Glass/ITO substrates (10 Ω sq^{-1} , Geomatec Co., Ltd.) were etched with zinc powder and HCl (6 M in deionized water), then consecutively cleaned with water, acetone, detergent solution (Semico Clean 56, Furuuchi chemical), water, and isopropyl alcohol with 15 min ultrasonic bath under each step. Before coating the PEDOT:PSS, plasma treatment was applied to clean the substrates. PEDOT:PSS aqueous dispersion was filtered through a 0.45 μm PTFE filter and then spin-coated on the ITO glass surface at 1000 rpm for 10 s and 4000 rpm for 30 s, and then annealed at 140 °C for 20 min under air. The substrates were transferred to an Ar-filled glove box (H_2O , $\text{O}_2 < 0.1$ ppm) and annealed at 140 °C for another 20 min. The perovskite layer was fabricated on PEDOT:PSS following the above-mentioned procedure. For EDAI_2 post-treatment, 1.0 mg EDAI_2 was added to 1.0

mL IPA and 1.0 mL toluene. The mixed solution was stirred at 70 °C for 3h and then filtered through a 0.20 μm PTFE filter before spin coating. After that, 150 μL solution was dynamically spin-coated onto perovskite films. The spin coating process was set as 4000 rpm for 20 s with an acceleration of 1333 rpm s⁻¹. Following spin coating, the films were immediately annealed at 70 °C for around 5 min. Subsequently, 15 mg mL⁻¹ solution of PCBM, OC or ICBA in CB/CS₂/TCB (10/5/1, v/v) was spin-coated at 2000 rpm for 30 s, followed by annealing at 70 °C for 10 min. 8 nm of bathocuproine (0.01 nm s⁻¹) was then deposited by thermal evaporation. Finally, 100 nm of Ag was deposited through a shadow mask to form the metal electrode. The deposition rate for Ag was set as 0.003 nm s⁻¹ until the thickness reached 5 nm, then 0.01 nm s⁻¹ until 20 nm, and finally 0.08 nm s⁻¹ until the target thickness was reached. The overlap area of the bottom ITO and the uppermost silver electrode of the devices was 0.15 cm².

The device for electron-only devices for SCLC (space-charge limited current) measurements adopted the device structures of glass/ITO/ZnO/ETM/BCP/Ag. ZnO was filtered through a 0.45 μm PTFE filter and then spin-coated on the plasma-treated ITO glass at 3000 rpm for 30 s, followed by thermal annealing at 200 °C for 30 min under air. After the samples were transferred to an Ar-filled glove box, 30 mg mL⁻¹ solution of PCBM, OC, or ICBA in CB/CS₂/TCB (10/5/1, v/v) was filtrated through 0.20 μm PTFE filters. The filtrated solutions were subsequently spin-coated at 2000 rpm for 30 s on the ITO/ZnO samples, followed by thermal annealing at 70 °C for 10 min. We note that the concentration of 30 mg mL⁻¹ is slightly higher than the solubility of OC in CB/CS₂/TCB (10/5/1, v/v) so the OC solution formed a saturated solution. Lastly, BCP and Ag were deposited using the same procedure employed for the fabrication of solar cells. The overlap area of the bottom ITO and the uppermost silver electrode of the devices is 0.15 cm².

For the measurements of photoluminescence (PL) and time-resolved photoluminescence (TRPL), the perovskite and perovskite/ETM samples were prepared using the same procedure employed for the fabrication of the solar cells, except the substrate was changed to plasma-treated quartz.

Characterization

Scanning electron microscopy (SEM) was performed with a Hitachi S8010 ultra-high-resolution scanning electron microscope (Hitachi High-Tech Corporation). Atomic force microscopy (AFM) was performed with a Picoscan Plus AFM instrument used in AC-mode with Nanoworld NCST probes. UV–vis absorption measurement was performed with a JASCO V-780 spectrophotometer.

Cyclic voltammetry (CV) of thin film was performed on an ALS/chi-620C electrochemical analyzer using a three-electrode cell with an ETMs-adsorbed ITO working electrode, a Pt wire counter electrode, and an Ag/AgNO₃ reference electrode. The films of ETMs were spin-coated on a plasma-treated ITO surface (condition: 15 mg mL⁻¹ CB/CS₂/TCB (10/5/1, v/v) solution of ETMs, 2000 rpm). The measurements were carried out using acetonitrile solution of 0.1 M tetrabutylammonium hexafluorophosphate (*n*Bu₄NPF₆) as a supporting electrolyte. The redox potentials were calibrated with ferrocene as an internal standard. The area of the working electrode dipped into the electrolyte solution is 0.9 cm × 1.25 cm. The measurement of CV in solutions was performed on an ALS/chi-620C electrochemical analyzer using a three-electrode cell with a glassy carbon working electrode, a platinum wire counter electrode, and an Ag/AgNO₃ reference electrode. The measurements were carried out using 1 mM solutions of ETMs and 0.1 M tetrabutylammonium tetrafluoroborate (TBABF₄) as a supporting electrolyte, and the potentials were calibrated with ferrocene used as an internal standard which was added after each measurement. The CV measurements were carried out under an argon atmosphere.

Photocurrent–voltage (*J–V*) curves were measured in an N₂-filled glove box (H₂O, O₂ <0.1 ppm) with an OTENTO-SUN-P1G solar simulator (Bunkoukeiki Co., Ltd.). The light intensity of the illumination source was calibrated using a standard silicon photodiode. The active area of the devices was 0.0985 cm² as defined by the aperture of the shadow mask placed between the light source and test cells.

Each device was measured with a 10-mV voltage step and a 100 ms time step (i.e., scan rate of 0.1 V s⁻¹) using a Keithley 2400 source meter.

External quantum efficiency (EQE) were measured with a Bunkoukeiki SMO-250III system equipped with a Bunkoukeiki SM-250 diffuse reflection unit (Bunkoukeiki Co.,

Ltd.). The incident light intensity was calibrated with a standard SiPD S1337-1010BQ silicon photodiode.

Impedance spectroscopy data was obtained with an E4990A impedance analyzer (Keysight) with an oscillator voltage of 30mV, in the frequency range of 20-200,000 Hz. The measurements were performed with the devices exposed to AM1.5G-equivalent radiation in an inert atmosphere, with a 0.1 cm² shadow mask. The impedance data was fit by a series resistor (r_s) along with a capacitor (c_p) in parallel with a resistor (r_p).

SCLC measurements were measured in the dark in a glove box with a Keithley 2400 source meter. The electrons were injected from BCP/Ag and collected at ITO/ZnO. The voltage was increased logarithmically scanning from low to high voltage. The SCLC

electron mobility of the ETMs was fitted using the Mott–Gurney equation^{2,3} $J = \frac{9}{8} \epsilon_0 \epsilon_r \mu_e V^2 d^{-3}$, where J , ϵ_0 , ϵ_r , μ_e , V , d are the current density of the device, vacuum permittivity (8.854×10^{-12} F/m), relative permittivity of the ETM, SCLC electron mobility, bias voltage, and the thickness of the ETM, respectively. The ϵ_r values were assumed to be 3 for all ETMs. The thicknesses were 77 nm, 67 nm, and 86 nm for PCBM, OC, and ICBA, respectively, determined based on their respective cross-sectional SEM images.

For the PL and TRPL measurements, the samples were excited from the substrate side by a picosecond pulsed light with a wavelength of 688 nm (Advanced Laser Diode System). The excitation fluence was set at 100 nJ cm⁻². The PL spectra were collected from the substrate side and were recorded using an N₂-cooled charge-coupled-device array equipped with a monochromator (Princeton Instruments). The TRPL signals were recorded using an avalanche photodiode (ID Quantique) and a time-correlated single photon counting board (PicoQuant). The TRPL traces were fitted with a double exponential function $PL(t) = A_1 \exp(-t/\tau_1) + A_2 \exp(-t/\tau_2)$, and the average PL lifetimes were calculated using the equation $\tau_{avg} = (A_1 \tau_1^2 + A_2 \tau_2^2)/(A_1 \tau_1 + A_2 \tau_2)$. During the measurement, the samples were kept in an Ar-filled metallic box with quartz windows to avoid oxygen contamination and degradation.

The ¹H measurements were carried out at room temperature (unless otherwise noted) with JEOL JNM ECA500 and Bruker Advance III 400 spectrometer. The NMR chemical shifts

were reported in ppm with reference to residual protons and carbons of acetone- d_6 (δ 2.05 ppm in ^1H NMR) and DMSO- d_6 (δ 2.50 ppm in ^1H NMR). Atmospheric pressure chemical ionization (APCI) mass spectra were measured on a Bruker micrOTOF-Q II. The high-performance liquid chromatography (HPLC) was performed with the use of a Cosmosil Buckyprep column (250 mm in length, 4.6 mm in inner diameter) for analytical purpose and the same columns (two directly connected columns; 250 mm in length, 20 mm in inner diameter) for preparative purpose. Column chromatography was performed using PSQ 60B (Fuji Silysia). XPS was recorded with a JPS-9010 (JEOLCo.,Ltd.) instrument, with an X-ray energy of 1.5 keV ($\text{Al K}\alpha$), a step of 0.1 eV, and a dwell time of 200 ms. The perovskite film samples were transferred to the XPS chamber through an Ar-filled transfer vessel in order to avoid oxygen contamination.

Computational Methods

Theoretical calculations were performed using the Gaussian 09 software package. Ground state structures were optimized at the B3LYP-D3/6-31G(d,p) level of theory without any symmetry assumptions and confirmed by frequency analyses at the same level of theory.

Synthesis of OC

The purity of OC in this study was confirmed by the ^1H NMR and MS data shown below.

Supplementary Figures and Tables

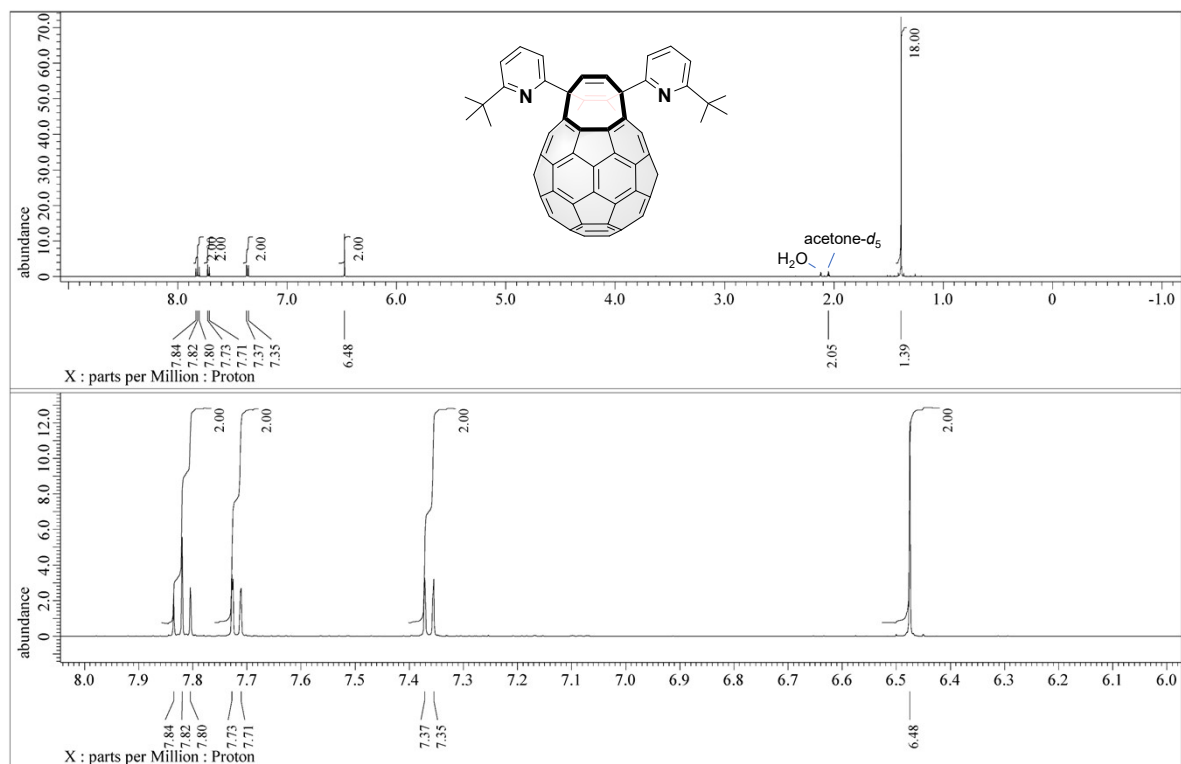


Figure S1. ^1H NMR spectra (500 MHz, $\text{CS}_2/\text{acetone-}d_6$ (5:1)) of OC.

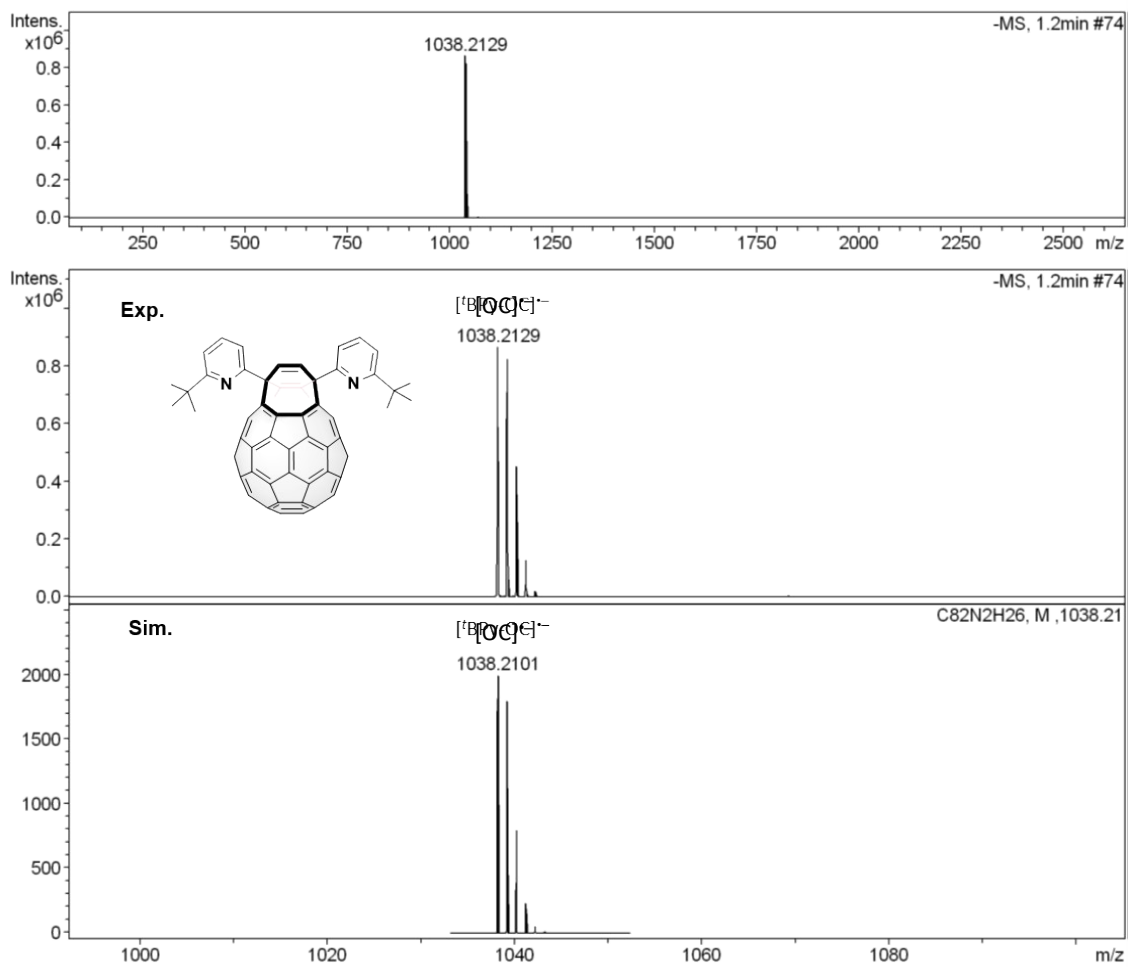


Figure S2. APCI mass spectra (negative ionization mode) of OC.

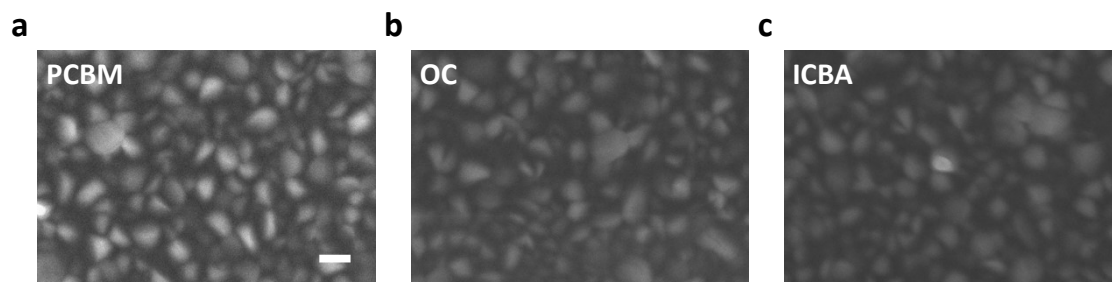


Figure S3. Top view SEM images of (a) PCBM, (b) OC, and (c) ICBA films grown on Sn-based perovskite layers (scale bar is 2 μm).

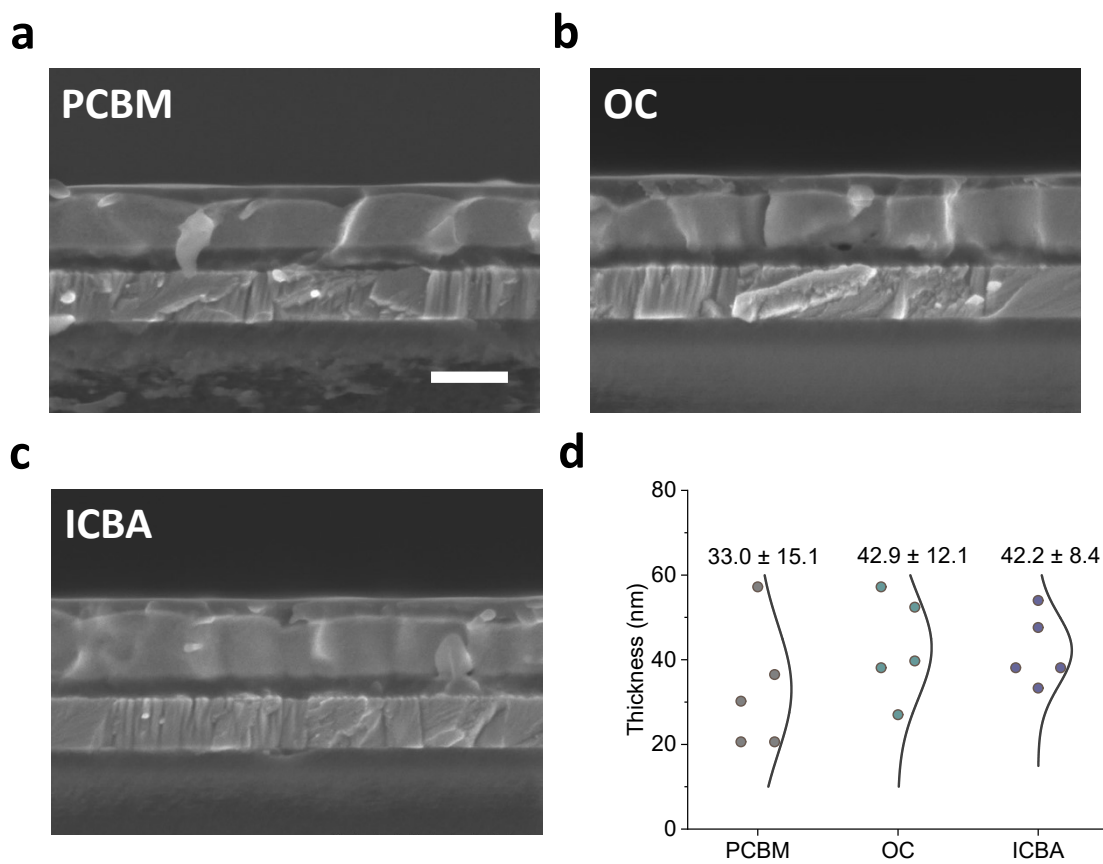


Figure S4. Cross section SEM images of (a) PCBM, (b) OC, and (c) ICBA films fabricated onto Sn-based perovskite layers (The scale bar is 500 nm). (d) The average thickness of the PCBM, OC and ICBA films estimated from SEM images.

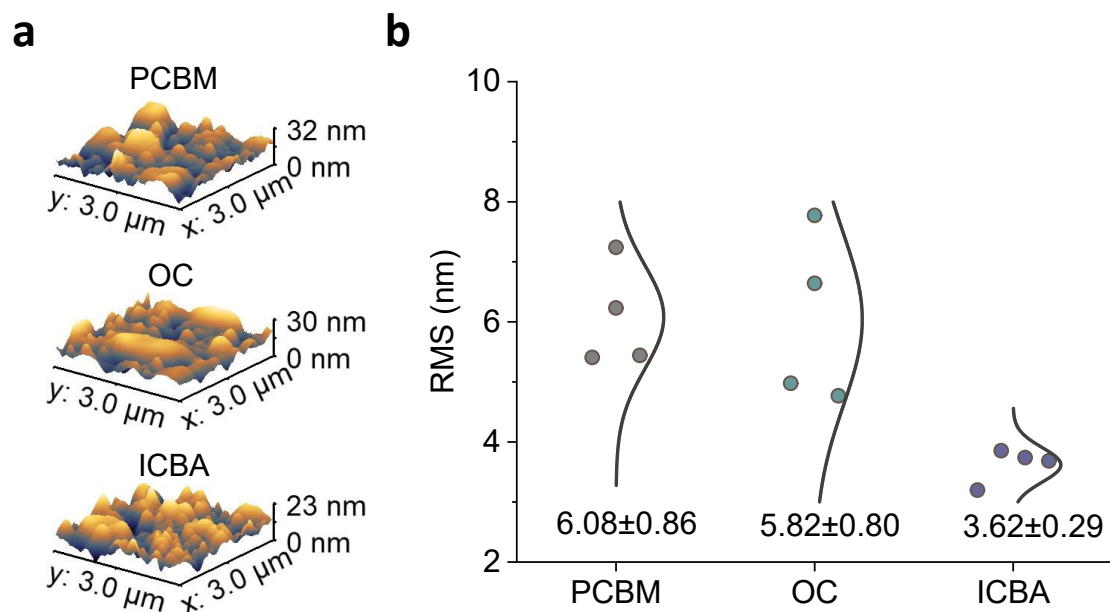


Figure S5. (a) AFM images and (b) the root-mean-square roughness of PCBM, OC and ICBA-covered perovskite samples.

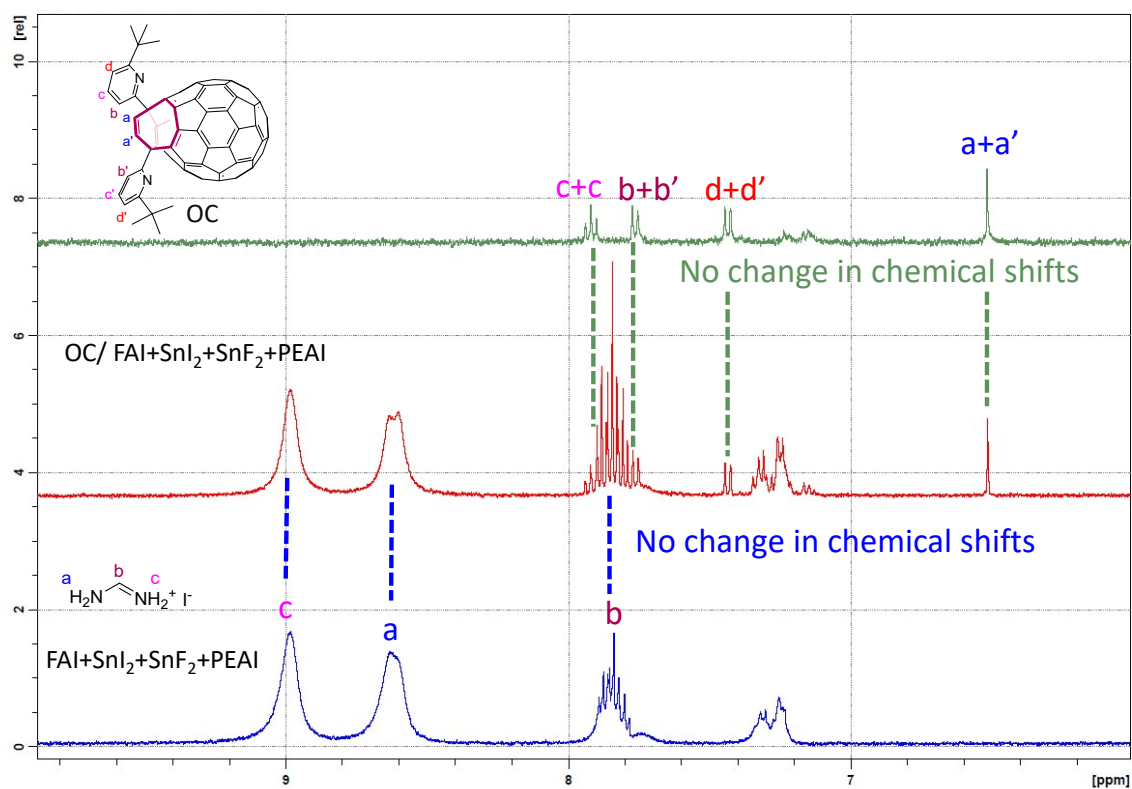


Figure S6. ^1H NMR spectra (500 MHz, $\text{DMSO-}d_6/\text{CS}_2(2:1)$) of OC, OC mixed with (FAI+SnI₂+SnF₂+PEAI), and mixture of (FAI+SnI₂+SnF₂+PEAI).

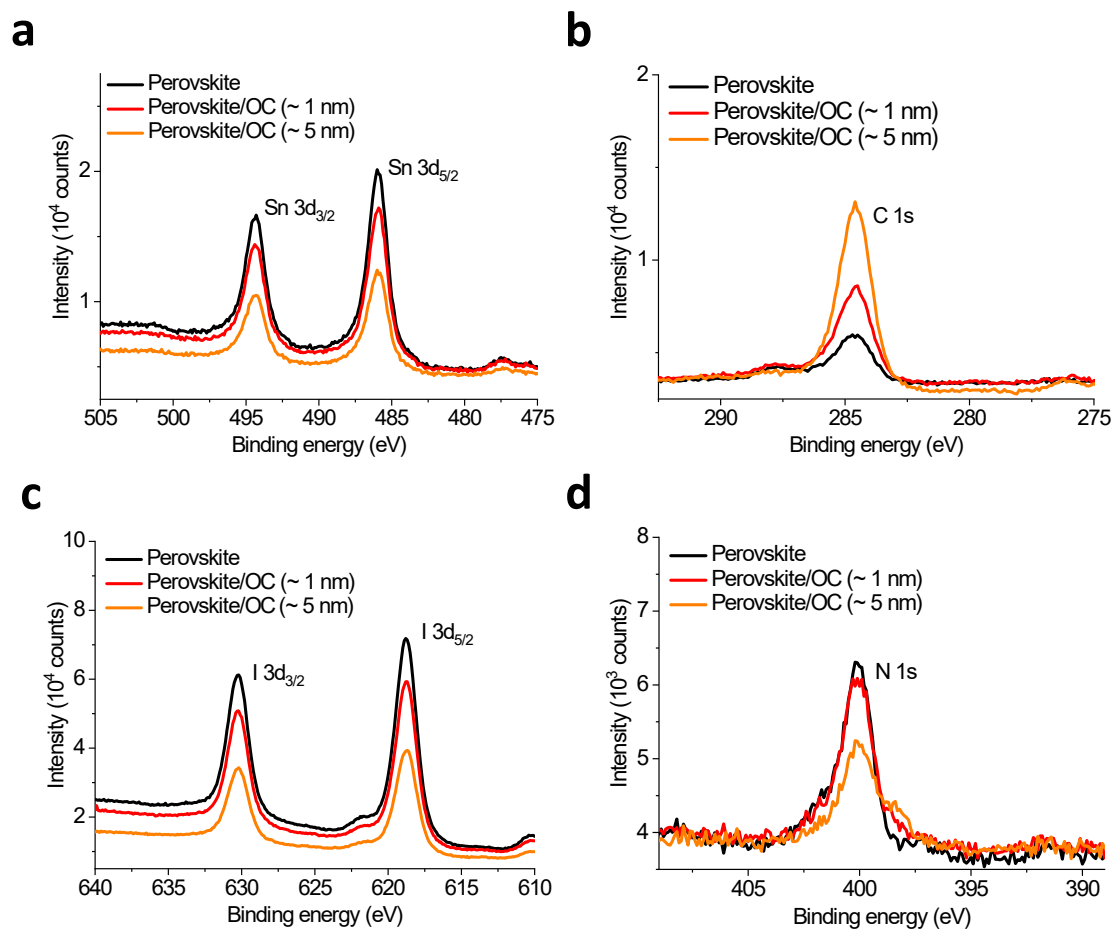


Figure S7. XPS spectra of the (a) Sn ($3d_{3/2}$ and $3d_{5/2}$), (b) C $1s$, (c) I ($3d_{3/2}$ and $3d_{5/2}$), and (d) N $1s$ core levels for the bare perovskite films and perovskite films treated with 1 or 5 nm OC.

Table S1. Champion and average PV parameters of PSCs from a single batch of six solar cells.

Molecule for ETM	J_{SC} (mA cm ⁻²) ^a	V_{OC} (V) ^a	FF ^a	PCE (%) ^a
PCBM	17.7 (18.4 ± 1.3)	0.57 (0.48 ± 0.04)	0.52 (0.48 ± 0.03)	5.3 (4.3 ± 0.5)
OC	19.6 (18.9 ± 0.7)	0.72 (0.69 ± 0.06)	0.68 (0.65 ± 0.04)	9.6 (8.5 ± 0.8)
ICBA	20.7 (20.3 ± 0.4)	0.82 (0.76 ± 0.05)	0.69 (0.67 ± 0.03)	11.6 (10.4 ± 0.7)

^a The average and standard deviation values are given in parentheses.

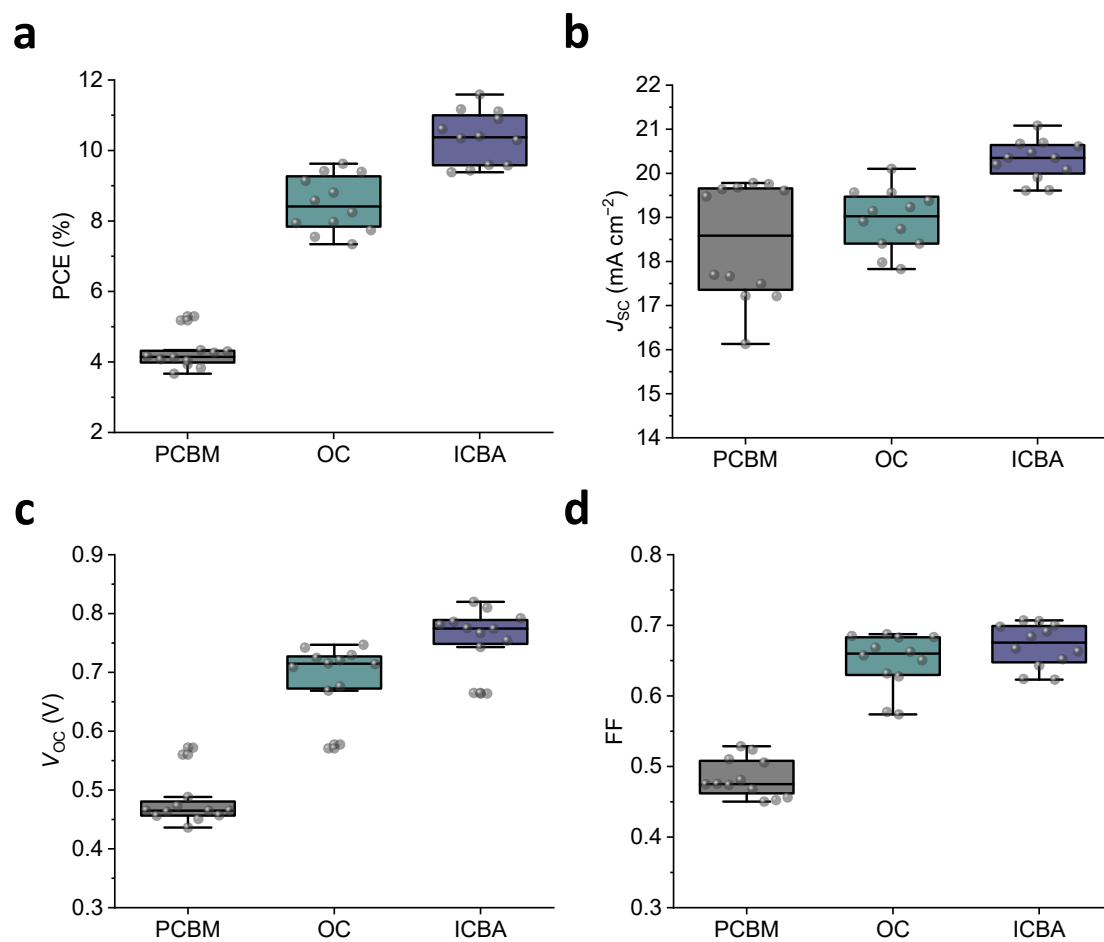


Figure S8. Distributions of (a) PCE, (b) J_{sc} , (c) V_{oc} , and (d) FF values derived for six devices with PCBM, OC, and ICBA. The data includes values derived from both forward and reverse J - V scans.

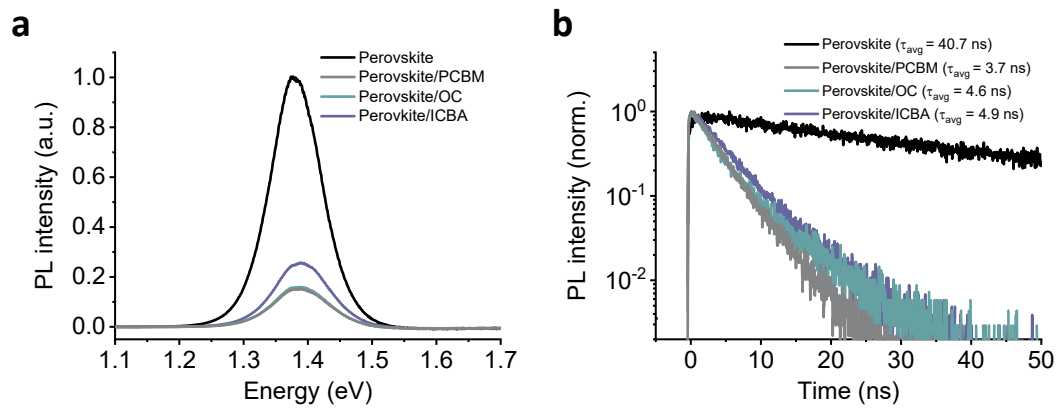


Figure S9. (a) PL and (b) TRPL spectra of perovskite and perovskite/ETM thin films deposited on quartz substrates. Here, the perovskite with ICBA on top shows the highest PL intensity and the longest TRPL lifetime, followed by those with OC and PCBM.

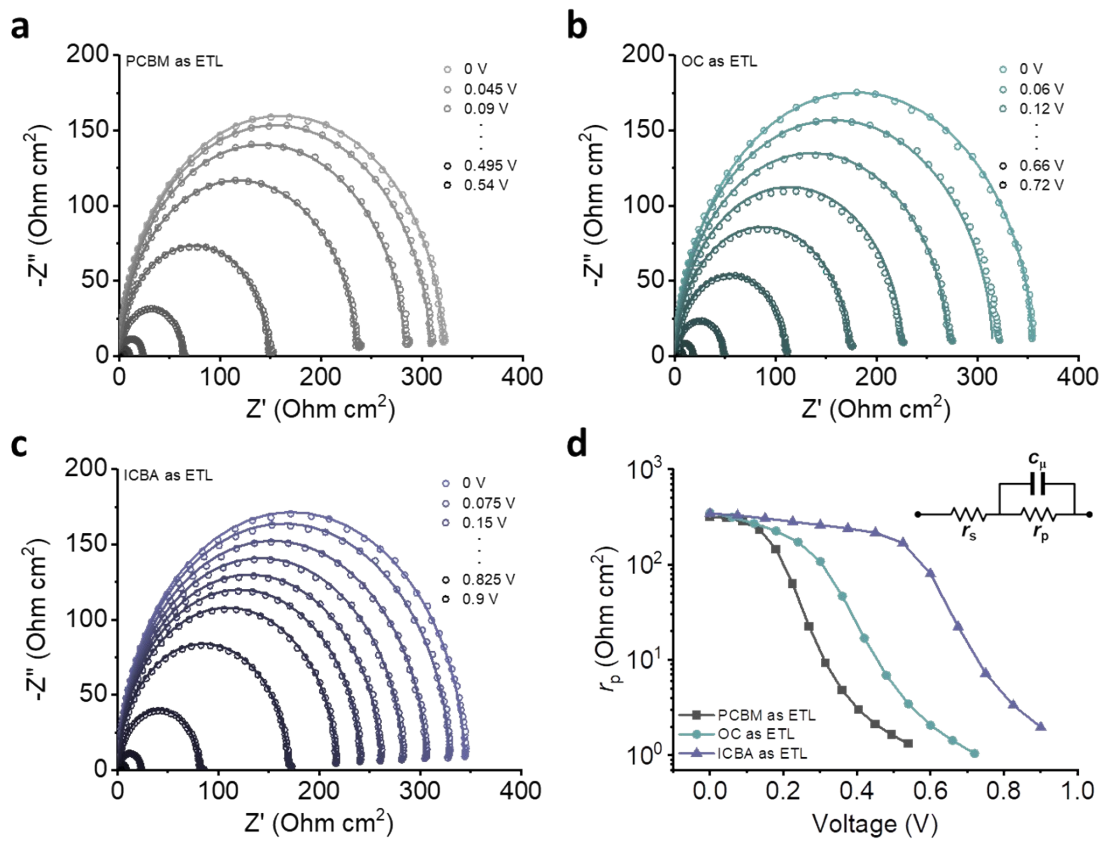


Figure S10. Impedance spectra of $\text{PEA}_{0.15}\text{FA}_{0.85}\text{SnI}_3$ solar cells using (a) PCBM, (b) OC, and (c) ICBA as ETMs under AM1.5G-equivalent radiation. Symbols and the solid lines represent the measured data and fitted results, respectively. (d) Fitted r_p as functions of bias voltage for the solar cells using PCBM, OC, and ICBA as ETMs. Inset: the equivalent circuit used to model the data. Here, r_s is governed by the measurement-related electrical contact, such as the electrodes of the devices, and the values of the r_s are almost identical ($\approx 1 \Omega \text{ cm}^2$) for all devices. r_p is inversely correlated with the degree of carrier recombination in the solar cells.

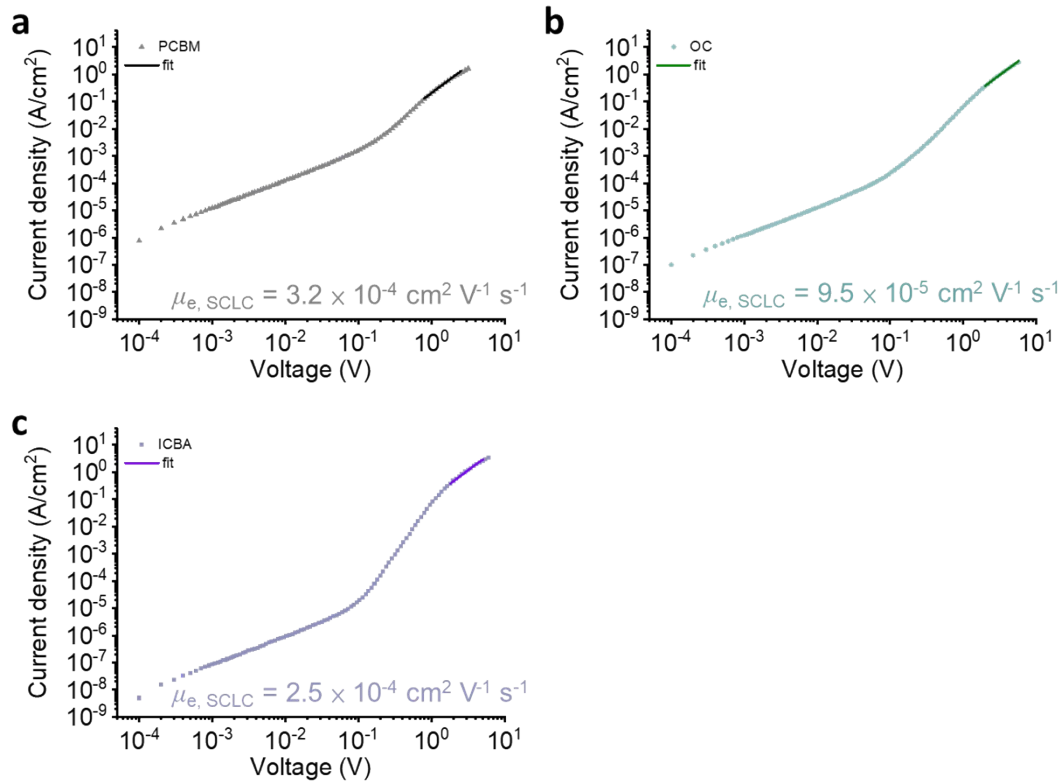


Figure S11. Dark J - V curves of the (a) PCBM-, (b) OC-, and (c) ICBA-based electron-only devices. Solid lines represent fit to the data according to Mott–Gurney equation $J \propto \mu_e V^2$, where μ_e and V stand for SCLC electron mobility and applied voltage, respectively. The SCLC electron mobility of the ETMs was fitted using the Mott–Gurney equation^{2,3}

$$J = \frac{9}{8} \varepsilon_0 \varepsilon_r \mu_e V^2 d^{-3}$$

where J , ε_0 , ε_r , μ_e , V , d are the current density of the device, vacuum permittivity (8.854×10^{-12} F/m), relative permittivity of the ETM, SCLC electron mobility, bias voltage, and the thickness of the ETM, respectively. The ε_r values were assumed to be 3 for all ETMs. The thicknesses were 77 nm, 67 nm, and 86 nm for PCBM, OC, and ICBA, respectively, determined based on their respective cross-sectional SEM images.

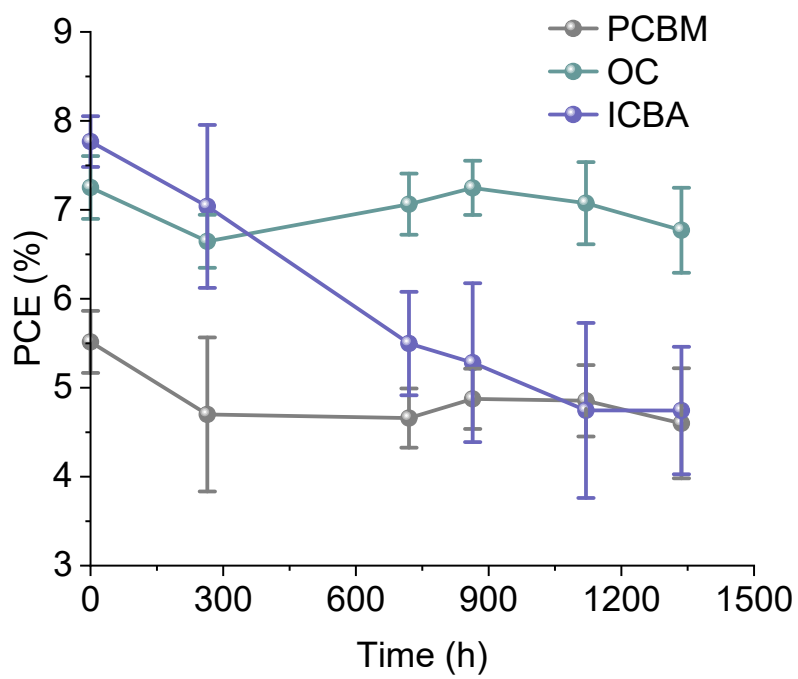
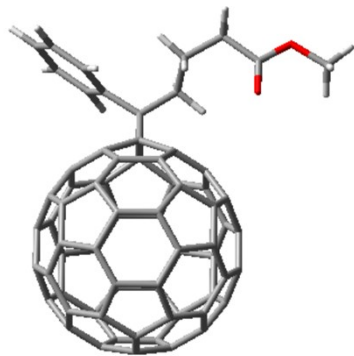


Figure S12. Shelf-stability of unencapsulated cells with PCBM, OC, and ICBA. For this test, devices were stored in the dark in an N₂-filled glove box. The error bars represent the standard deviation. The data includes values derived from both forward and reverse $J-V$ scans of three devices for each ETM.

Table S2. Optimized geometry of PCBM (B3LYP-D3/6-31G(d,p)).

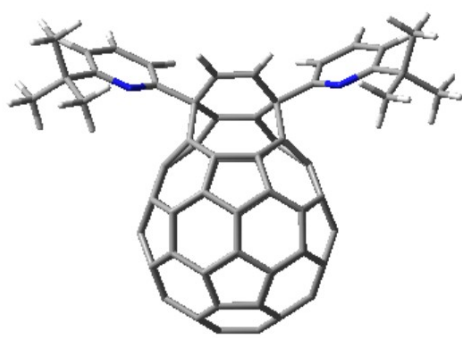


Standard orientation:

Center Number	Atomic Number	Atomic Type	Coordinates (Angstroms)		
			X	Y	Z
1	8	0	4.645292	-3.076925	0.464821
2	8	0	6.690016	-3.672116	-0.286818
3	6	0	2.074149	0.851686	-1.024500
4	6	0	2.235488	0.586561	0.563325
5	6	0	1.427233	1.478250	1.446103
6	6	0	0.709911	2.566930	0.977432
7	6	0	0.563306	2.809561	-0.470872
8	6	0	1.140628	1.955533	-1.396972
9	6	0	0.377922	1.537927	-2.548141
10	6	0	0.670208	0.141438	-2.811704
11	6	0	1.618236	-0.321400	-1.827194
12	6	0	1.483191	-1.596796	-1.300336
13	6	0	1.631624	-1.839091	0.147956
14	6	0	1.910876	-0.798633	1.018669
15	6	0	1.189005	-0.708968	2.264873
16	6	0	0.894372	0.687298	2.527716
17	6	0	-0.297104	1.044107	3.164703
18	6	0	-1.033446	2.193876	2.695273
19	6	0	-0.541692	2.930249	1.611973
20	6	0	-1.457027	3.396292	0.585258
21	6	0	-0.776495	3.316556	-0.695497
22	6	0	-1.495632	2.953016	-1.839165
23	6	0	-0.903617	2.040446	-2.788561
24	6	0	-1.947005	1.161769	-3.292049
25	6	0	-1.665983	-0.180209	-3.545007
26	6	0	-0.329712	-0.700473	-3.305028
27	6	0	-0.450448	-2.040529	-2.780279
28	6	0	0.434281	-2.471745	-1.786484
29	6	0	-0.065174	-3.251107	-0.667424
30	6	0	0.671125	-2.857230	0.521153
31	6	0	0.013045	-2.799346	1.754151
32	6	0	0.278442	-1.697162	2.648175
33	6	0	-0.967479	-1.325093	3.299322
34	6	0	-1.249232	0.016538	3.553501
35	6	0	-2.584188	0.538126	3.317691
36	6	0	-2.450266	1.885751	2.786637
37	6	0	-3.326147	2.333847	1.797344
38	6	0	-2.819465	3.109886	0.676444
39	6	0	-3.561517	2.720099	-0.512039
40	6	0	-2.912195	2.643948	-1.744586
41	6	0	-3.191974	1.535570	-2.643969
42	6	0	-4.106882	0.548473	-2.273120
43	6	0	-3.813816	-0.851491	-2.537173
44	6	0	-2.617331	-1.208658	-3.161478
45	6	0	-1.864735	-2.359851	-2.688265
46	6	0	-2.341200	-3.107419	-1.610789
47	6	0	-1.421310	-3.567643	-0.582474
48	6	0	-2.105703	-3.494158	0.698534
49	6	0	-1.401880	-3.117565	1.842967
50	6	0	-2.009085	-2.205630	2.799765

51	6	0	-3.292663	-1.706086	2.571928	87	1	0	5.358858	-5.037266	-1.143652
52	6	0	-3.586162	-0.306233	2.836073	88	1	0	7.040493	-5.590091	-0.836658
53	6	0	-4.497512	0.163061	1.807027	-----					
54	6	0	-4.370496	1.457597	1.299649	The total electronic energy E was calculated to be -2902.51156006 Hartree. The					
55	6	0	-4.516076	1.696438	-0.128281	frequency calculations using the optimized structure showed no imaginary frequency. The					
56	6	0	-4.783076	0.631017	-0.990213	LUMO level is -0.10977 a.u. (-2.99 eV).					
57	6	0	-4.909817	-0.717012	-0.461227						
58	6	0	-4.770011	-0.946097	0.907908						
59	6	0	-4.023647	-2.100586	1.380324						
60	6	0	-3.441582	-2.977881	0.463383						
61	6	0	-3.587369	-2.739026	-0.964608						
62	6	0	-4.308928	-1.632572	-1.417011						
63	6	0	3.399148	1.000992	-0.306877						
64	6	0	3.941205	2.398578	-0.145681						
65	6	0	4.179114	3.185024	-1.279345						
66	6	0	4.745924	4.453084	-1.156903						
67	6	0	5.082415	4.949830	0.104593						
68	6	0	4.849111	4.172021	1.239838						
69	6	0	4.280634	2.903403	1.114464						
70	6	0	4.478019	-0.048285	-0.587367						
71	6	0	5.379955	-0.316474	0.623738						
72	6	0	6.414913	-1.410372	0.349867						
73	6	0	5.790721	-2.785124	0.190658						
74	6	0	6.200196	-5.015979	-0.445160						
75	1	0	3.906539	2.801082	-2.259078						
76	1	0	4.919578	5.055013	-2.044763						
77	1	0	5.519815	5.939717	0.201943						
78	1	0	5.104364	4.553070	2.224912						
79	1	0	4.087968	2.303130	1.998876						
80	1	0	4.015279	-0.987347	-0.897569						
81	1	0	5.079673	0.309123	-1.433478						
82	1	0	4.755893	-0.622499	1.471188						
83	1	0	5.899151	0.603526	0.913861						
84	1	0	7.007871	-1.192188	-0.546710						
85	1	0	7.135786	-1.479401	1.175422						
86	1	0	5.870355	-5.420659	0.515898						

Table S3. Optimized geometry of OC (B3LYP-D3/6-31G(d,p)).



18	6	0	-0.004399	-2.099851	-3.276554
19	6	0	-1.102461	-2.797185	-2.936165
20	6	0	-2.180583	-2.145177	-2.461239
21	6	0	-2.845097	-2.651712	-1.407115
22	6	0	-2.449932	-3.804963	-0.837140
23	6	0	-1.366834	-4.448737	-1.312680
24	6	0	-0.690086	-3.943341	-2.360895
25	6	0	0.657796	-3.950540	-2.358127
26	6	0	1.324850	-4.463127	-1.307198
27	6	0	2.412840	-3.830966	-0.827249
28	6	0	0.647204	-4.973175	-0.261252
29	6	0	-0.698953	-4.965988	-0.263992
30	6	0	1.319076	-4.661590	0.863524
31	6	0	0.646578	-4.353847	1.988129
32	6	0	-0.700862	-4.346643	1.985395
33	6	0	-1.372016	-4.647200	0.858051
34	6	0	-2.452916	-3.925676	0.504101
35	6	0	-2.847787	-2.893622	1.273751
36	6	0	-2.186310	-2.598796	2.404807
37	6	0	-1.115279	-3.331690	2.767841
38	6	0	-0.021018	-2.722196	3.261357
39	6	0	1.068639	-3.343355	2.772243
40	6	0	2.148936	-2.621983	2.413579
41	6	0	2.811846	-2.923895	1.285247
42	6	0	2.409076	-3.951684	0.513990
43	6	0	3.181000	-1.760918	0.717927
44	6	0	2.723269	-0.725952	1.445664
45	6	0	2.136637	-1.279890	2.525439
46	6	0	1.066112	-0.672757	3.050367
47	6	0	-0.014158	-1.386611	3.406961
48	6	0	-1.085262	-0.661232	3.046019
49	6	0	-2.160098	-1.256914	2.516770
50	6	0	-2.736290	-0.696806	1.434568

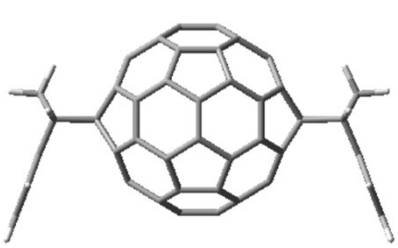
Standard orientation:

Center Number	Atomic Number	Atomic Type	Coordinates (Angstroms)		
			X	Y	Z
1	6	0	1.610116	1.521316	-1.074288
2	6	0	0.695527	0.984794	-1.931577
3	6	0	-0.676917	0.992180	-1.934432
4	6	0	-1.589252	1.538540	-1.080927
5	6	0	-2.378559	0.611112	-0.468902
6	6	0	-2.756902	-0.475781	-1.168583
7	6	0	-2.157456	-0.804356	-2.321192
8	6	0	-1.053652	-0.107128	-2.621818
9	6	0	0.002353	-0.769462	-3.099471
10	6	0	1.063399	-0.118466	-2.617428
11	6	0	2.158486	-0.827395	-2.312299
12	6	0	2.756930	-0.505158	-1.157381
13	6	0	2.387451	0.585783	-0.459224
14	6	0	3.188564	-1.650966	-0.613890
15	6	0	2.822590	-2.681980	-1.395545
16	6	0	2.167816	-2.168384	-2.452336
17	6	0	1.084748	-2.808850	-2.931668

51	6	0	-3.202175	-1.726792	0.704948	87	1	0	3.858080	5.580231	2.487188
52	6	0	-3.203097	-1.616838	-0.626882	88	1	0	5.914815	4.879627	1.361321
53	6	0	-2.330730	0.482515	0.895813	89	1	0	-5.860861	4.951211	1.345054
54	6	0	-1.330457	1.146493	1.544745	90	1	0	-3.794777	5.645079	2.457239
55	6	0	-0.674609	0.502148	2.525083	91	1	0	-1.670904	4.628764	1.731779
56	6	0	0.670022	0.494914	2.527792	92	1	0	1.256715	4.513270	-1.649260
57	6	0	1.336670	1.132097	1.550084	93	1	0	-7.447734	3.263581	1.040397
58	6	0	2.332602	0.457652	0.905285	94	1	0	-7.981563	2.103984	-0.206086
59	6	0	-0.663220	2.124661	0.904025	95	1	0	-6.621779	1.674796	0.888567
60	6	0	0.682504	2.117325	0.906717	96	1	0	-5.040668	2.355381	-2.514842
61	6	0	1.403314	2.756310	-0.236538	97	1	0	-6.663589	1.652002	-2.262373
62	6	0	-1.372485	2.771146	-0.242269	98	1	0	-5.300713	1.099272	-1.246383
63	6	0	-0.643118	3.826052	-1.012538	99	1	0	-7.054440	5.089098	-0.759019
64	6	0	2.683182	3.402947	0.273432	100	1	0	-6.003761	4.735287	-2.172903
65	6	0	2.668750	4.301983	1.271386	101	1	0	-7.617604	3.957193	-2.023472
66	6	0	3.828234	4.841575	1.669948	102	1	0	5.061596	2.378658	-2.542927
67	6	0	4.949783	4.452762	1.047388	103	1	0	6.672132	1.639834	-2.309608
68	6	0	4.875959	3.551640	0.051670	104	1	0	5.298259	1.080578	-1.312846
69	6	0	-2.646069	3.433255	0.263900	105	1	0	6.616605	1.571056	0.843263
70	7	0	-3.727585	3.103056	-0.305922	106	1	0	7.990935	2.007575	-0.230194
71	6	0	-4.838414	3.598076	0.048184	107	1	0	7.468251	3.140236	1.046560
72	6	0	-4.900917	4.511500	1.033410	108	1	0	6.073348	4.728466	-2.132789
73	6	0	-3.774043	4.896997	1.648334	109	1	0	7.128288	5.020400	-0.707894
74	6	0	-2.620743	4.342468	1.252393	110	1	0	7.669907	3.912498	-2.001572
75	7	0	3.759847	3.069714	-0.303723						
76	6	0	0.688611	3.819236	-1.009362						
77	6	0	-6.074939	3.100583	-0.699123						
78	6	0	-7.081705	2.508535	0.310180						
79	6	0	-5.747134	1.996632	-1.732141						
80	6	0	-6.720570	4.283281	-1.449917						
81	6	0	6.105577	3.051907	-0.705397						
82	6	0	5.760729	1.984421	-1.770719						
83	6	0	7.094962	2.412890	0.292190						
84	6	0	6.778376	4.241368	-1.421103						
85	1	0	-1.201064	4.525894	-1.655000						
86	1	0	1.723022	4.591545	1.756795						

The total electronic energy E was calculated to be -3249.90224688 Hartree. The frequency calculations using the optimized structure showed no imaginary frequency. The LUMO level is -0.10769 a.u. (-2.93 eV).

Table S4. Optimized geometry of ICBA (*trans*-1) (B3LYP-D3/6-31G(d,p)).



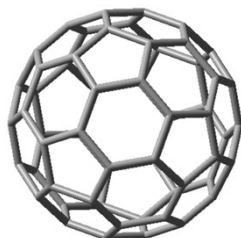
Standard orientation:

Center Number	Atomic Number	Atomic Type	Coordinates (Angstroms)		
			X	Y	Z
1	6	0	-2.948313	1.491151	1.396319
2	6	0	-2.432373	2.503505	0.673596
3	6	0	-2.432380	2.503512	-0.673574
4	6	0	-2.948346	1.491175	-1.396316
5	6	0	-2.186654	1.044042	-2.416165
6	6	0	-1.091069	1.705245	-2.832892
7	6	0	-0.673774	2.803545	-2.181113
8	6	0	-1.345804	3.186705	-1.082567
9	6	0	-0.672195	3.608389	0.000021
10	6	0	-1.345800	3.186708	1.082610
11	6	0	-0.673766	2.803522	2.181156
12	6	0	-1.091065	1.705215	2.832919
13	6	0	-2.186630	1.044006	2.416191
14	6	0	0.000013	1.040788	3.253338
15	6	0	1.091123	1.705162	2.832921
16	6	0	0.673881	2.803481	2.181139
17	6	0	1.345942	3.186658	1.082615
18	6	0	0.672375	3.608384	0.000017
19	6	0	1.345945	3.186680	-1.082585
20	6	0	0.673886	2.803527	-2.181121
21	6	0	1.091121	1.705207	-2.832917
22	6	0	2.186660	1.043942	-2.416177
23	6	0	2.948354	1.491065	-1.396316
24	6	0	2.432488	2.503448	-0.673579
25	6	0	2.432502	2.503432	0.673604
26	6	0	2.948386	1.491038	1.396329
27	6	0	2.186677	1.043907	2.416191
28	6	0	3.744499	0.366940	0.770589
29	6	0	3.744481	0.366943	-0.770570
30	6	0	2.949568	-0.753087	1.400875
31	6	0	2.432826	-1.762738	0.674022
32	6	0	2.432818	-1.762714	-0.674048
33	6	0	2.949538	-0.753067	-1.400876
34	6	0	2.187068	-0.304228	-2.418694
35	6	0	1.091168	-0.965225	-2.834727
36	6	0	0.673803	-2.062956	-2.181846
37	6	0	1.345654	-2.445172	-1.082727
38	6	0	0.672146	-2.866481	-0.000020
39	6	0	1.345655	-2.445196	1.082702
40	6	0	0.673800	-2.062987	2.181824
41	6	0	1.091167	-0.965268	2.834718
42	6	0	2.187078	-0.304268	2.418702
43	6	0	-0.000019	-0.300532	3.254127
44	6	0	-1.091245	-0.965233	2.834729
45	6	0	-0.673946	-2.062977	2.181838
46	6	0	-1.345809	-2.445172	1.082713
47	6	0	-0.672322	-2.866475	-0.000014
48	6	0	-1.345813	-2.445151	-1.082733
49	6	0	-0.673951	-2.062952	-2.181863
50	6	0	-1.091250	-0.965189	-2.834739
51	6	0	-0.000030	-0.300481	-3.254130

52	6	0	0.000007	1.040841	-3.253333	75	6	0	-6.660325	-3.062725	0.673129
53	6	0	-2.187119	-0.304141	-2.418700	76	6	0	-6.224541	-1.995703	1.365264
54	6	0	-2.949598	-0.752942	-1.400878	77	6	0	5.798170	1.273880	0.000005
55	6	0	-2.432921	-1.762613	-0.674049	78	6	0	-5.797976	1.274010	0.000033
56	6	0	-2.432917	-1.762636	0.674019	79	1	0	-5.499827	0.674014	2.176114
57	6	0	-2.949578	-0.752960	1.400870	80	1	0	-5.499838	0.674069	-2.176100
58	6	0	-2.187101	-0.304165	2.418703	81	1	0	5.499867	0.674043	2.176103
59	6	0	-3.744481	0.367073	-0.770580	82	1	0	5.499858	0.674040	-2.176098
60	6	0	-3.744467	0.367068	0.770567	83	1	0	6.212206	-1.985799	2.465961
61	6	0	-5.239095	0.384303	1.138824	84	1	0	7.018255	-3.952384	1.218333
62	6	0	-5.239097	0.384318	-1.138820	85	1	0	7.018189	-3.952356	-1.218430
63	6	0	-5.794973	-0.937634	-0.668561	86	1	0	6.212102	-1.985751	-2.466000
64	6	0	-5.794947	-0.937643	0.668553	87	1	0	-6.212218	-1.985807	-2.465977
65	6	0	5.795004	-0.937670	0.668555	88	1	0	-7.018412	-3.952301	-1.218362
66	6	0	5.239141	0.384281	1.138826	89	1	0	-7.018360	-3.952317	1.218365
67	6	0	5.239134	0.384290	-1.138817	90	1	0	-6.212119	-1.985824	2.465971
68	6	0	5.794973	-0.937649	-0.668549	91	1	0	5.385308	2.307192	0.000008
69	6	0	6.224567	-1.995720	1.365259	92	1	0	6.911228	1.332880	-0.000001
70	6	0	6.660224	-3.062772	0.673106	93	1	0	-5.384789	2.307199	0.000025
71	6	0	6.660205	-3.062785	-0.673179	94	1	0	-6.910995	1.333321	0.000032
72	6	0	6.224503	-1.995705	-1.365313						
73	6	0	-6.224578	-1.995693	-1.365278						
74	6	0	-6.660356	-3.062718	-0.673143						

The total electronic energy E was calculated to be -2981.92613841 Hartree. The frequency calculations using the optimized structure showed no imaginary frequency. The LUMO level is -0.10753 a.u. (-2.92 eV).

Table S5. Optimized geometry of C₆₀ (B3LYP-D3/6-31G(d,p)).



Standard orientation:

Center Number	Atomic Number	Atomic Type	Coordinates (Angstroms)		
			X	Y	Z
1	6	0	0.779447	1.878968	-2.908465
2	6	0	0.069726	0.809541	-3.455544
3	6	0	0.647318	-0.524052	-3.449958
4	6	0	1.911880	-0.734984	-2.899444
5	6	0	2.651717	0.379287	-2.330467
6	6	0	2.096399	1.659337	-2.334423
7	6	0	2.223544	2.510796	-1.163287
8	6	0	0.984745	3.256455	-1.013637
9	6	0	0.092108	2.865652	-2.092220
10	6	0	-1.277508	2.743843	-1.855532
11	6	0	-2.016753	1.629425	-2.424882
12	6	0	-1.356957	0.682231	-3.208788
13	6	0	-1.661143	-0.730327	-3.050895
14	6	0	-0.422533	-1.475890	-3.200657
15	6	0	-0.184980	-2.600012	-2.409071
16	6	0	1.132072	-2.819563	-1.834884
17	6	0	2.159185	-1.906189	-2.075068
18	6	0	3.051719	-1.515875	-0.996331
19	6	0	3.355936	-0.103308	-1.154014
20	6	0	3.477891	0.713952	-0.029564
21	6	0	2.899910	2.047619	-0.034269
22	6	0	2.365593	2.310795	1.291836
23	6	0	1.176402	3.026472	1.435573
24	6	0	0.471854	3.508526	0.259123
25	6	0	-0.954853	3.381315	0.506082
26	6	0	-1.811963	3.007075	-0.529591
27	6	0	-2.881400	2.054809	-0.279390
28	6	0	-3.007787	1.203450	-1.450690
29	6	0	-3.299880	-0.152497	-1.299391
30	6	0	-2.612692	-1.139236	-2.115918
31	6	0	-2.365610	-2.310843	-1.291724
32	6	0	-1.176413	-3.026508	-1.435464
33	6	0	-0.471848	-3.508699	-0.259106
34	6	0	0.954886	-3.381262	-0.506163
35	6	0	1.811963	-3.007059	0.529515
36	6	0	2.881385	-2.054802	0.279387
37	6	0	3.007800	-1.203419	1.450631
38	6	0	3.299897	0.152498	1.299304
39	6	0	2.612843	1.139248	2.116044
40	6	0	1.661146	0.730303	3.050833
41	6	0	0.422509	1.475875	3.200570
42	6	0	0.184952	2.600127	2.409201
43	6	0	-1.132086	2.819593	1.834788
44	6	0	-2.159170	1.906235	2.075011
45	6	0	-3.051692	1.515862	0.996325
46	6	0	-3.355917	0.103322	1.153947
47	6	0	-3.477882	-0.713890	0.029500
48	6	0	-2.900077	-2.047700	0.034315
49	6	0	-2.223528	-2.510730	1.163268
50	6	0	-0.984707	-3.256392	1.013600
51	6	0	-0.092090	-2.865864	2.092256
52	6	0	1.277489	-2.743861	1.855461

53	6	0	2.016802	-1.629388	2.424870
54	6	0	1.357135	-0.682243	3.208950
55	6	0	-0.069743	-0.809554	3.455460
56	6	0	-0.779432	-1.878952	2.908490
57	6	0	-2.096602	-1.659429	2.334510
58	6	0	-2.651768	-0.379309	2.330440
59	6	0	-1.911872	0.735054	2.899444
60	6	0	-0.647369	0.524174	3.450103

The total electronic energy E was calculated to be -2285.953805 Hartree. The frequency calculations using the optimized structure showed no imaginary frequency. The LUMO level is -0.11848 a.u. (-3.22 eV).

References

- (1) K. Kurotobi and Y. Murata, *Science*, 2011, **333**, 613–616.
- (2) J. Dacuña, *Phys. Rev. B*, 2011, **84**, 195209.
- (3) J. C. Blakesley, F. A. Castro, W. Kylberg, G. F. A. Dibb, C. Arantes, R. Valaski, M. Cremona, J. S. Kim and J.-S. Kim, *Org. Electron.*, 2014, **15**, 1263–1272.